Supramolecular properties of amphiphilic adamantylated azo dyes

Supramolecular properties of amphiphilic adamantylated azo dyes

*Filip Zatloukal, Eva Achbergerová, David Gergela, Michal Rouchal, Lenka Dastychová, Zdeňka Prucková and Robert Vícha**

Department of Chemistry, Faculty of Technology, Tomas Bata University in Zlín, Vavrečkova 275, 760 01 Zlín, Czech Republic

Email: rvicha@utb.cz; Tel.: +420 576031103

Abstract

Despite environmental and health risks, azo dyes are still very popular colourising agents; therefore, methods for removing the dyes and/or related pollutants from wastewater have been developed. We have incorporated a lipophilic adamantane cage into two polar disulphonatonaphthalene-1-azobenzene dyes to prove the concept that modified dyes can be treated via host–guest supramolecular interactions using suitable cyclodextrin (CD) and cucurbit[*n*]uril (CB*n*) hosts. We conducted ^{1}H NMR experiments to demonstrate that both dyes form specific inclusion complexes with an adamantane cage buried inside the CB7 or β-CD cavity. Using isothermal titration calorimetry, we determined association constants with β-CD and CB7 in the range of (0.7–1.3) × 10^{6} and (1.4–3.4) × 10^{8}, respectively. As the dye@CB7 complexes were sparingly soluble in water, the dye can be efficiently removed from water by precipitation, even in the presence of β-CD.

Keywords: azo dye; adamantane; host–guest complex; supramolecular properties

Highlights

- Synthesis of amphiphilic azo dyes bearing adamantane moiety.

- Formation of highly stable host–guest complexes with β-cyclodextrin (log K≈6).
- Formation of 100 × stronger host–guest complexes with cucurbit[7]uril (log K≈8).
- Up to 99 % of dye can be precipitated by two equivalents of cucurbit[7]uril.

Graphical abstract

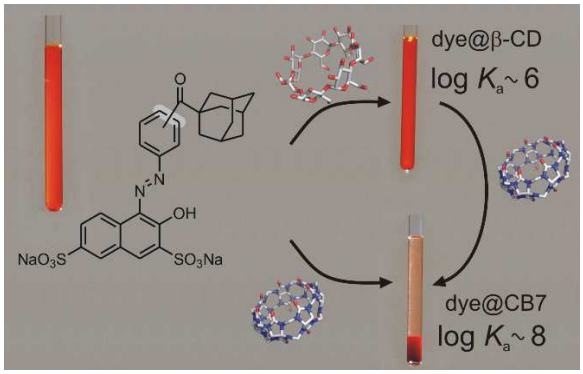

1. Introduction

Azo compounds are widely used in the chemical industry as dyes, pigments [1], additives, indicators [2], therapeutic agents [3] and initiators of radical reactions [4]. Their usage in electronics is promising [5], and they have been conjugated with biomacromolecules to construct drug delivery systems [6]. Recently, research has focused on potential applications of azo compounds in the fields of non-linear optics, optical storage media, chemosensors, liquid crystals [7], photochemical molecular switches [8], molecular transporters [9], nanotubes [10] and the production of protective eyewear and filters [11].

Azo compounds represent one of the most important groups of dyes in the 160-year history of synthetic dyes [12]. Compared to natural dyes, synthetic dyes are of low cost, characterised by a wide range of colours, easy to dye and highly stable as a product. However, they can also cause serious environmental and health risks, such as groundwater pollution from industrial dyes and their by-products, which has become a serious environmental problem [13].

Recently, supramolecular chemistry has provided opportunities for dye stabilisation, immobilisation and removal from wastewater, and there are two highly recognised and popular host families: cyclodextrins (CDs) and cucurbit[*n*]urils (CB*n*s).

Cyclodextrins are natural compounds obtained by the enzymatic degradation of starch. Cyclic oligosaccharides α-CD, β-CD and γ-CD consist of six, seven and eight glucose units, respectively. Macrocycles adopt the shape of a hollow cone with a hydrophobic central cavity and hydrophilic rims decorated with hydroxyl groups [14,15]. The hydrophobic cavity can catch or encapsulate other molecules of a non-polar nature [15,16,17]. The second family of host molecules, cucurbit[*n*]urils, are macrocyclic compounds consisting of *n* glycoluril units that are connected by 2*n* of methylene bridges [18,19]. Molecules of cucurbit[*n*]urils are highly symmetrical and barrel-shaped with a hydrophobic cavity and polar portals lined with carbonyl groups [20]. The utilisation of these compounds is somewhat limited by low water solubility [19], but the ability to form extremely stable inclusion complexes is their indisputable advantage [20b].

The combination of azo dye as a guest and cyclodextrins or cucurbit[*n*]urils as hosts has led to the publication of several interesting supramolecular systems in recent years. Thus, Harada designed a photoswitchable sol–gel system based on curdlan that was functionalised with α-CD and an azo-modified poly(acrylic acid) as a guest polymer [21]. Other authors described the preparation of a β-CD dimer consisting of azobenzene moiety as a linker [22]. A photoisomerisation study with an ethylenediaminetetraacetic acid (EDTA) derivative guest bearing two adamantane moieties indicated that this dimer can form two different inclusion complexes with the guest. *Cis*-isomer encapsulated two adamantyl units into both cavities forming a 1:1 cyclic complex, while the *trans*-isomer formed a supramolecular polymer with an *n*:*n* stoichiometry. Additionally, many other dyes were modified with an adamantane cage to employ the host–guest approach. For instance, the adamantane cage was linked to perylene

dye to form supramolecular aggregates [23]. The lipophilic adamantane cage affected the biodistribution of the dye to allow for the selective staining of cell organelles [24]. Adamantane–cyclodextrin complexation was used as a tool to modulate the fluorescence of squaraine dyes [25]. Fluorescent polymeric nanoparticles based on a cyclodextrin-modified polymer and adamantylated dye were developed for biological imaging [26]. Finally, the cucurbit[*n*]urils [27] and cyclodextrins [28] displayed an ability to precipitate some commercial dyes, such as methylene blue, methyl orange and oil orange SS, respectively. In the light of these examples, it is surprising that no adamantane-modified azo dyes have been reported so far, to the best of our knowledge.

As previously indicated, adamantane is the favoured binding motif for dye modifications to allow for the construction of supramolecular host–guest systems. Adamantane-modified dyes benefit from the fact that the adamantane cage perfectly fits into the CB7 and β-CD cavity to form highly stable host–guest complexes. Therefore, we prepared two amphiphilic dyes consisting of adamantylcarbonylphenyl lipophilic scaffold, which is linked via the azo group to polar naphthalenedisulphonate moiety (Figure 1). We tested the supramolecular properties of the new dyes on cyclodextrins and cucurbit[*n*]urils using NMR, titration calorimetry and mass spectrometry.

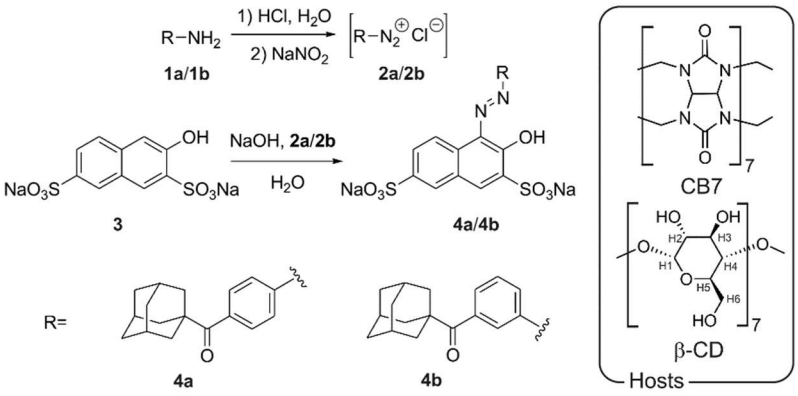

Figure 1 Dyes and macrocyclic hosts considered in this study

2. Materials and methods

General

All of the solvents, reagents and starting compounds were of analytical grade and were purchased from commercial sources; they were used without further purification, if not stated otherwise. Adamantylanilines **1a** and **1b** were prepared following a previously published procedure [29]. Melting points were measured on a Kofler block. Elemental analyses (C, H, N and S) were performed using a Thermo Fisher Scientific Flash EA 1112. NMR spectra were recorded using a Bruker Avance III 500 spectrometer operating at frequencies of 500.11 MHz (^{1}H) and 125.77 MHz (^{13}C), and a Jeol JNM-ECZ400R/S3 spectrometer operating at frequencies of 399.78 MHz (^{1}H) and 100.53 MHz (^{13}C). ^{1}H- and ^{13}C-NMR chemical shifts were referenced to the signal of the solvent [^{1}H: δ(residual DMSO-d_5) = 2.50 ppm, δ(residual HDO) = 4.70 ppm; ^{13}C: δ(DMSO-d_6) = 39.52 ppm]. The mixing time for ROESY was adjusted to 200 ms for **4a** and 150 ms for **4b**. Signal multiplicity is indicated by 's' for singlet, 'd' for doublet, 'm' for multiplet and 'um' for unresolved multiplet. IR spectra were recorded using a Smart OMNI-Transmission Nicolet iS10 spectrophotometer. The samples were measured in KBr pellets. UV–Vis spectra were recorded using a Thermo Spectronic UNICAM UV 500. Electrospray mass spectra (ESI-MS) were recorded using an amaZon X ion-trap mass spectrometer (Bruker Daltonics, Bremen, Germany) equipped with an electrospray ionisation source. All of the experiments were conducted in the negative-ion polarity mode. The instrumental conditions used to measure the single azo dyes and their mixtures with the host molecules were different; therefore, they are described separately. *Single dyes*: Individual samples (with concentrations of 0.5 μg·cm^{-3}) were infused into the ESI source in methanol:water (1:1, v:v) solutions using a syringe pump with a constant flow rate of 3 μl·min^{-1}. The other instrumental conditions were as follows: an electrospray voltage of +4.2 kV, a capillary exit voltage of −140 V, a drying gas temperature of 220°C, a drying gas flow

rate of 6.0 $dm^3 \cdot min^{-1}$ and a nebuliser pressure of 55.16 kPa. *Host–guest complexes*: An MeOH:water (1:1, v:v) solution of the guest (10 μM) or an aqueous solution, in the case of CB7/8, and the equimolar amount of the corresponding host was infused into the ESI source at a constant flow rate of 3 $\mu l \cdot min^{-1}$. The other instrumental conditions were as follows: an electrospray voltage of +4.0 kV, a capillary exit voltage of −140 V, a drying gas temperature of 300°C, a drying gas flow rate of 6.0 $dm^3 \cdot min^{-1}$ and a nebuliser pressure of 206.84 kPa. Nitrogen was used as both the nebulising and drying gas for all of the experiments. Tandem mass spectra were collected using collision-induced dissociation (CID) with He as the collision gas after the required ions were isolated. Isothermal titration calorimetry measurements were carried out in H_2O using a VP-ITC MicroCal instrument at 303 K. The concentrations of the host in the cell and the guest in the microsyringe were approximately 0.04 mM and 0.40 mM, respectively. The raw experimental data were analysed with MicroCal ORIGIN software. The heats of dilution were taken into account for each guest compound. The data were fitted to a theoretical titration curve using the one set of sites model, and a competitive approach[30] was employed if needed. The *K* values obtained from the competitive titrations were verified using two different concentrations of the competitor. All titrations were performed in triplicate.

2.1. Synthesis

General protocol for the synthesis of compounds **4a/4b**

The reaction mixture was prepared in three portions. The first portion contained a mixture of $NaNO_2/H_2O$ (Mixture A), the second portion consisted of 1-adamantyl(aminophenyl)ketone **1a/1b** which was dissolved in 6 M HCl (Mixture B), and the third portion contained 3-hydroxynapthalene-2,7-disulphonic acid disodium salt (**3**) and $NaOH/H_2O$ (Mixture C). All mixtures were cooled to 0 °C. Mixture A was added to Mixture B using a cold Pasteur pipette and stirred for 15 min to form diazonium salt **2a/2b** *in situ*. The obtained solution was

transferred into Mixture C and stirred for 15 min. The final product was filtered, washed with EtOAc and dried.

4-(2-(4-(1-adamantylcarbonyl)phenyl)diazenyl)-3-hydroxynaphthalene-2,7-disulphonate disodium salt (**4a**)

The title compound was prepared according to the general procedure from the following materials: 1-adamantyl(4-aminophenyl)methanone (**1a**, 103 mg; 0.40 mmol), 3-hydroxynapthalene-2,7-disulphonic acid disodium salt (**3**, 140 mg; 0.40 mmol), $NaNO_2$ (29 mg; 0.42 mmol), NaOH (343 mg; 8.58 mmol) and 6 M HCl (530 µl). The pure product **4a** was obtained as a red powder in yield 189 mg (76 %). M.p.: >340 °C; ε(25 °C, H_2O, λ = 492 nm) = (15.75 ± 0.16) × 10^3 $dm^3 \cdot mol^{-1} \cdot cm^{-1}$. Calcd. for $C_{27}H_{24}N_2Na_2O_8S_2 \cdot 1.8\ H_2O$ C 50.12, H 4.30, N 4.33, S 9.91. Found C 49.93, H 4.37, N 4.52, S 10.23. ^{1}H NMR (400 MHz, D_2O): δ1.78 (um, 6H), 2.02 (um, 6H), 2.10 (um, 3H), 4.69 (s, 1H), 7.45 (d, 2H, $^3J_{H,H}$ = 8.6 Hz), 7.59 (d, 2H, $^3J_{H,H}$ = 8.7 Hz), 7.88 (d, 1H, $^4J_{H,H}$ = 1.4 Hz), 8.00 (dd, 1H, $^3J_{H,H}$ = 8.7 Hz, $^4J_{H,H}$ = 1.4 Hz), 8.18 (s, 1H), 8.43 (d, 1H, $^3J_{H,H}$ = 8.6 Hz) ppm. ^{1}H NMR (400 MHz, DMSO[d_6]): δ1.73 (um, 6H), 1.99 (um, 6H), 2.05 (um, 3H), 7.75 (d, 2H, $^3J_{H,H}$ = 8.4 Hz), 7.83 (3H), 7.92 (s, 1H), 8.24 (s, 1H), 8.41 (d, 1H) ppm. ^{13}C NMR (101 MHz, DMSO[d_6]): δ27.6, 36.0, 38.7, 46.2, 118.2, 120.9, 126.3, 126.8, 128.1, 129.2, 130.2, 136.0, 141.5, 141.6, 207.1 ppm. IR (KBr, disc): 3448 (s,b), 2904 (s), 2849 (s), 1660 (m), 1613 (m), 1599 (m), 1552 (m), 1499 (s), 1478 (m), 1453 (w), 1271 (m), 1197 (s), 1156 (m), 1108 (m), 1054 (m) 1038 (s), 997 (m), 987 (m), 930 (m), 841 (m), 710 (m) 676 (m) 644 (m) 573 (w) cm^{-1}. ESI-MS (neg.) *m/z* (%): 283.9 $[M–2\cdot Na^+]^{2–}$ (100), 591.0 $[2\cdot(M–Na^+)^–]^{2–}$ (4).

4-(2-(3-(1-adamantylcarbonyl)phenyl)diazenyl)-3-hydroxynaphthalene-2,7-disulphonate disodium salt (**4b**)

The title compound was prepared according to the general procedure from the following materials: 1-adamantyl(3-aminophenyl)methanone (**1b**, 110 mg; 0.43 mmol), 3-hydroxynapthalene-2,7-disulphonic acid disodium salt (**3**, 150 mg; 0.43 mmol), $NaNO_2$ (30 mg; 0.43 mmol), NaOH (343 mg; 8.58 mmol), and 6M HCl (570 µl). The pure product **4b** was obtained as a red powder in yield 169 mg (71 %). M.p.: >340 °C; ε(25 °C, H_2O, λ = 488 nm) = (15.14 ± 0.02) × 10^3 $dm^3 \cdot mol^{-1} \cdot cm^{-1}$. Calcd. for $C_{27}H_{24}N_2Na_2O_8S_2 \cdot 1.5\ H_2O$ C 50.54, H 4.24, N 4.37, S 10.00. Found C 50.39, H 4.28, N 4.42, S 9.88. ^{1}H NMR (400 MHz, D_2O): δ 1.72 (m, 6H), 1.92 (um, 6H), 2.03 (um, 3H), 4.69 (s, 1H), 7.33 (d, 1H, $^3J_{H,H}$ = 7.6 Hz), 7.46 (dd, 1H), 7.78 (d, 1H, $^3J_{H,H} \approx 9$ Hz), 7.80 (s, 1H); 7.93 (dd, 1H, $^3J_{H,H}$ = 8.6, $^4J_{H,H}$ = 1.8 Hz), 8.13 (d, 1H, $^4J_{H,H}$ = 1.7 Hz), 8.41 (d, 1H, $^3J_{H,H}$ = 8.5 Hz); 8.45 (s, 1H) ppm. ^{1}H NMR (400 MHz, DMSO[d_6]): δ 1.73 (um, 6H), 1.99 (um, 6H), 2.05 (um, 3H), 7.52 (d, 1H, $^3J_{H,H}$ = 7.5 Hz), 7.62 (dd, 1H, $^3J_{H,H}$ = 7.6 Hz); 7.81 (dd, 1H, $^3J_{H,H}$ = 7.8 Hz, $^4J_{H,H}$ = 1.4 Hz), 7.91 (um, 1H), 7.97 (s, 1H), 7.98 (m, 1H, $^3J_{H,H}$ = 8.4 Hz), 8.28 (s, 1H), 8.39 (d, 1H, $^3J_{H,H}$ = 8.4 Hz) ppm. ^{13}C NMR (101 MHz, DMSO[d_6]): δ 27.5, 35.9, 38.4, 46.2, 116.8, 119.6, 120.9, 125.4, 126.5, 127.4, 129.7, 129.9, 133.2, 138.5, 140.3, 140.8, 146.3, 171.0, 208.4 ppm. IR (KBr, disc): 3445 (s, b), 3068 (m), 2904 (s), 2850 (s), 1667 (m), 1615 (m), 1552 (m), 1504 (m), 1476 (m), 1453 (m), 1384 (m), 1267 (m), 1217 (s), 1191 (s, b), 1107 (m), 1056 (m), 1037 (s), 993 (m), 711 (m), 678 (m), 642 (m), 583 (m) cm^{-1}. ESI-MS (neg.) *m/z* (%): 283.9 $[M–2 \cdot Na^+]^{2–}$ (100), 591.0 $[2 \cdot (M–Na^+)^–]^{2–}$ (4).

3. Results and discussion

3.1 Synthesis

Starting adamantylated anilines were prepared according to a previously published procedure [29]. A slightly modified protocol, which was previously published by Anderson et al., was adopted for preparing the final azo dyes [31]. We decided to use 3-hydroxynaphthalene-2,7-disulphonate as a nucleophilic partner in the final step. This choice was motivated by two

aspects. First, it has been demonstrated that this bulky group serves as a stopper for β-CD in rotaxane structures [31], so there should be insignificant (if any) binding of the naphthalene part of the dye inside the β-CD cavity to simplify the interpretation of supramolecular experiments. Second, highly polar disulphonate groups increase the polarity of the dyes to allow for in-solution studies. Unlike many other substances described in recent literature [32], compounds **4a** and **4b** displayed only one tautomer form in D_2O solutions to enable an unambiguous interpretation of the experimental data that were obtained within the supramolecular experiments.

3.2 Isothermal Titration Calorimetry (ITC) results

To quantify the binding strength of our dyes with selected macrocyclic hosts, we determined association constants using titration calorimetry. The results are summarised in Table 1. Since the typical association constants (K) for adamantane derivatives with β-CD are of the order 10^5 in magnitude, we were surprised that the K values of our dyes reached the order of 10^6 to attack the most stable 1:1 complexes of β-CD [33]. We speculated that the aromatic linker between the azo moiety and the adamantane cage played an important role in stabilising the complex as it extends the hydrophobic part of the guest. However, additional stabilisation interactions between the cyclodextrin rim and polar part of the ligand also contribute because the highest K value, which was reported previously for similar ligands having an adamantylcarbonylphenyl binding motif, did not exceed 5.4×10^5 [34]. We also attempted to determine the stability of the complexes with α-CD using ITC. However, any reasonable data analysis was disabled due to a lack of heat evolution.

Subsequently, we tested two members of the cucurbit[n]uril family that have a sufficiently large interior cavity, i.e. CB7 and CB8. It is well known that the adamantane cage perfectly fits the CB7 interior cavity to gain a binding strength related to the log K value of 8–10 [20]. This value matches those reported in Table 1 to indicate that the adamantane cage is bound inside

206 the CB7 cavity by hydrophobic effect. It is worth noting that the interaction between **4a** and
207 CB7 displayed negative entropy, unlike the **4b** dye and other cage hydrocarbon derivatives [35].
208 We attributed this behaviour to the higher degree of conformational motions that were disabled
209 upon complexation in dye **4a**. This hypothesis is supported by the broad peaks observed in the
210 ^{13}C NMR spectrum of the **4a** dye (Figure S3). Lower *K* values, which were observed for
211 dye@CB8 complexes, were attributed to the wider cavity of the CB8 macrocycle.
212 Considering *K* values, we can infer that our adamantylated dyes are firmly bound in β-
213 cyclodextrin; however, they can be taken from these complexes by CB7, which can compete
214 with β-CD because it has approximately 100 × higher affinity.

215 **Table 1** Thermodynamic parameters obtained by ITC in water at 303 K

Guest	Host	*n*	*K*	$-\Delta H$ [kJ·mol^{-1}]	$T\Delta S$ [kJ·mol^{-1}]	$-\Delta G$ [kJ·mol^{-1}]
4a	β-CD	1.07±0.02	(1.34±0.08)×10^6	47±4	−11±4	35.6±0.1
	CB7	1.00±0.05	(1.38±0.04)×10^8 [a]	74±2	−27.0±1.8	47.2±1.2
	CB8	0.98±0.09	(3.6±0.3)×10^6	37±4	−4.2±1.2	38.1±0.2
4b	β-CD	0.93±0.02	(6.9±0.4)×10^5	52±2	−18.2±1.8	33.9±0.1
	CB7	0.99±0.03	(3.4±0.5)×10^8 [b]	44±6	5.5±1.5	49.5±7.8
	CB8	1.01±0.03	(5.2±0.5)×10^6	45±2	−5.8±1.5	39.0±0.2

216 Competitors were used as follows: [a] cyclopentanone K_{CB7}=3.91×10^5; [b] L-phenylalanine K_{CB7}=4.91×10^5

217 *3.3 ^{1}H NMR studies*

218 Continuing our study, we performed ^{1}H NMR titration experiments with β-CD and CB7 to
219 support previous ITC experiments with structural data. It is well known that the interior
220 environment of macrocyclic host molecules influences the chemical shifts of nuclei positioned
221 inside the cavities. It was previously demonstrated that H-atoms of the adamantane cage, which
222 are complexed inside the β-CD cavity, are markedly deshielded, whereas those inside the CB7
223 cavity are significantly shielded to display downfield or upfield complexation-induced shift
224 (CIS), respectively [20a]. The result of the ^{1}H NMR titration of dye **4a** with β-CD is shown in
225 Figure 2. The unambiguous downfield shift of the adamantane H-atom signals, particularly
226 H(b), indicates that the adamantane cage is buried inside the β-CD cavity within the complex.

It was already mentioned that the naphthyl group is too bulky to be included inside β-CD.

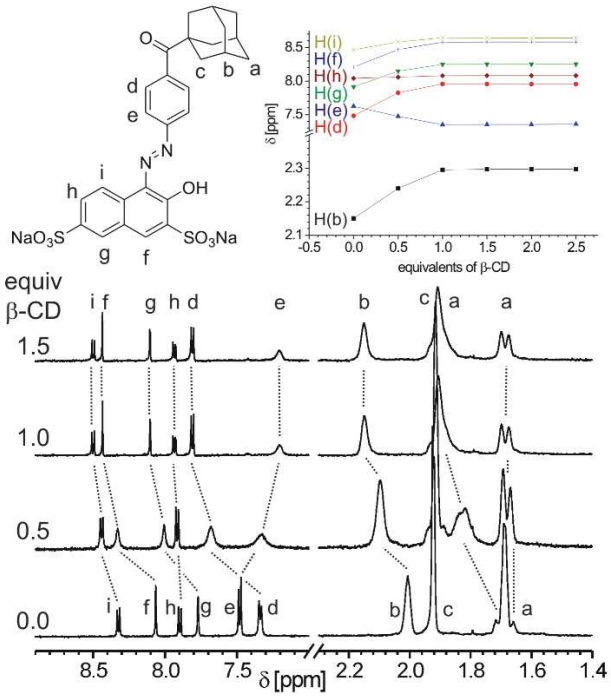

Figure 2 Portions of ^{1}H NMR spectra (400 MHz, D_2O, 303 K) recorded within titration of dye **4a** with β-CD.

Therefore, the significantly large CISs of the naphthyl H-atoms are somewhat surprising. We conjectured that N-atoms of the azo group and/or O-atom at position 3 on the naphthalene ring, which can act as H-bond acceptors, are positioned near the β-CD rim within the complex to induce the redistribution of electron density on the aromatic rings. Additionally, positioning the adamantane cage inside the β-CD cavity was supported by a ROESY experiment. As seen in Figure 3, clear cross-peaks were observed that indicate the spatial proximity of the inner H-atoms of β-CD (H3, H5, H6) and H-atoms of the adamantane cage H(a–c).

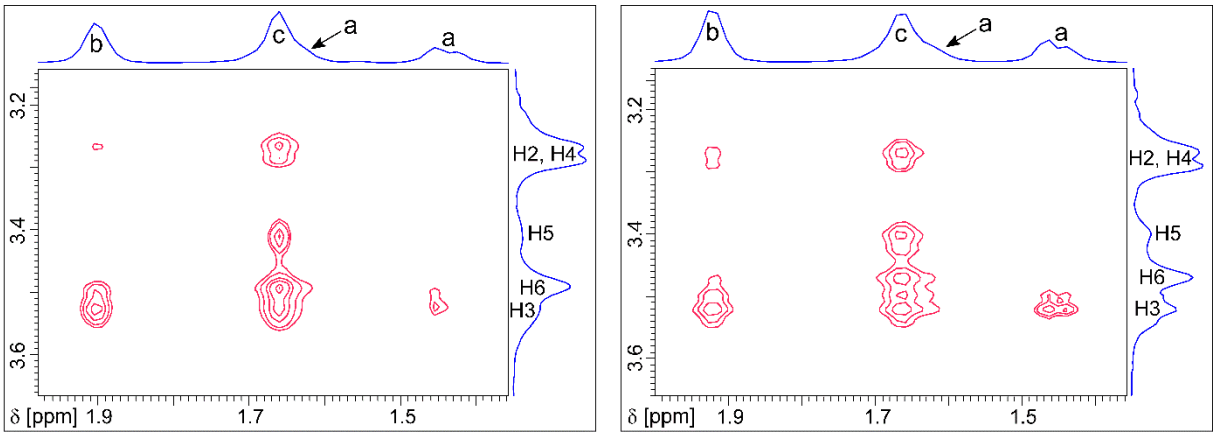

238

239 **Figure 3** Portions of the ROESY spectra (400 MHz, D_2O, 303 K) of β-CD with guests **4a** and **4b** from left to

240 right. The labelling of the guest and β-CD H-atoms corresponds to that in Figures 1, 2 and 4, respectively.

241 In the case of titrations with CB7, two sets of signals appeared in the spectra until an

242 equimolar ratio was reached. This phenomenon is related to the formation of a complex in a

243 slow exchange manner, according to the NMR timescale (500 MHz). A significant upfield shift

244 of adamantane H-atom signals, as shown in Figure 4, concerts with the hypothesis that the

245 adamantane cage is included inside the CB7 cavity. Downfield shift, which was observed for

246 all of the aromatic H-atoms, indicates that the aromatic part of the dye is positioned outside the

247 macrocycle close to the cavity portal. As Figure 4 demonstrates, the signal/noise ratio rapidly

248 decreased during titration to indicate a decrease in complex concentration due to precipitation.

249 This behaviour induced us to quantify the amount of dye that could be removed from the

250 solution by precipitation of the complex.

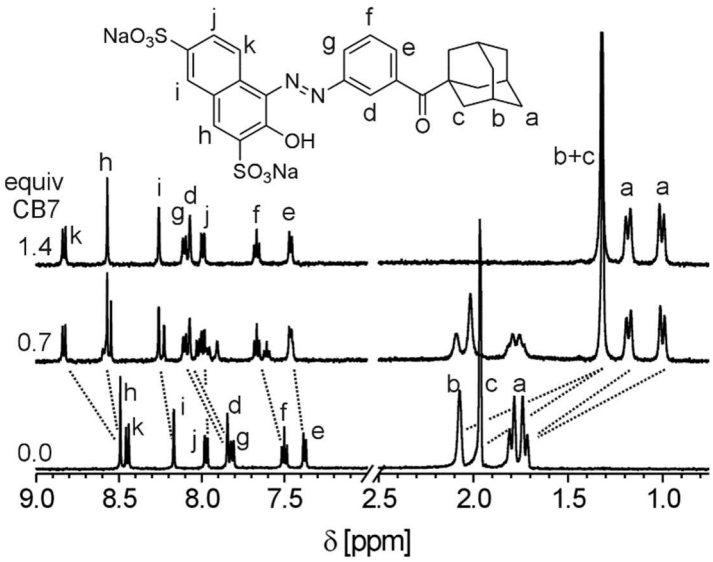

Figure 4 Portions of ^{1}H NMR spectra (500 MHz, D_2O, 303 K) recorded within the titration of dye **4b** with CB7.

^{1}H NMR was employed to determine the concentration of the dye remaining in the solution using maleic acid as an internal standard. Initially, we proved that maleic acid does not form a stable supramolecular complex with CB7 or β-CD under experimental conditions (D_2O, 303 K). Subsequently, we stepwise added two portions of approximately 1 equivalent of CB7 to the dye solution while maintaining an invariable concentration of maleic acid. After each addition, we calculated the total concentration of the dye in the solution. The results, which are summarised in Table 2, indicate that both dyes can be removed from the solution via the formation of a sparingly soluble supramolecular complex with CB7. However, the complex **4a**@CB7 was markedly less soluble than complex **4b**@CB7. No signals of dye were observed in the ^{1}H NMR spectrum of the **4a** mixture with approximately 2 equivalents of CB7 (Figure S14, line iv) to indicate that all of the dye was complexed with CB7 to form a insoluble complex. The presence of competing β-CD, which forms a soluble complex, did not significantly affect precipitation, and approximately 95% of the **4a** dye was removed. In terms of the more soluble **4b**, 90% and 75% of the dye was precipitated in the absence and presence of β-CD, respectively. The ^{1}H NMR spectra recorded within the precipitation experiment with the **4a** dye are given in Figure S14, along with snapshots depicting the physical appearance of the samples.

Table 2 Decrease in dye concentration [%] upon addition of CB7

The decrease in dye concentration [%]			
Dye	β-CD [equiv]	CB7 [equiv]	
		~1.1	~2.4
4a	0.0	83	>99
4a	1.1	50	95
4b	0.0	48	90
4b	1.1	44	75

3.4 Mass spectrometry

Finally, we used soft-ionising electrospray mass spectrometry to characterise supramolecular aggregates of the dyes and macrocyclic hosts. As the molecules of our dyes contain sulphonate functional groups, we employed negative ionisation mode to observe the desired complexes. Figure 5a shows a typical result of the measurement of the dye/β-CD mixture. The most abundant signal *m/z* 851.2, which can be attributed to the molecular doubly charged anion complexed with β-CD (hereinafter referred to as $[M^{2-}+\beta\text{-CD}]^{2-}$), was accompanied by signals *m/z* 284.1, *m/z* 1133.3 and *m/z* 1169.3 assigned to the molecular dianion and deprotonated β-CD and $[\beta\text{-CD}+Cl^-]^-$, respectively. The assignment of $[M^{2-}+\beta\text{-CD}]^{2-}$ was supported by collision-induced dissociation (CID) treatment. Figure 5b shows the precursor ion *m/z* 851.2 decomposition to $[M-2\cdot Na^+ + H^+]^-$ at *m/z* 569.1 and deprotonated β-CD at *m/z* 1133.3.

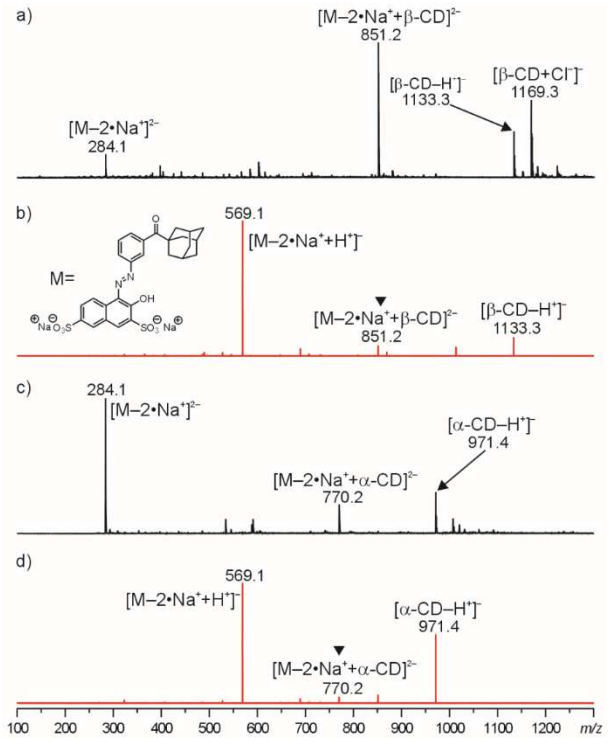

Figure 5 The negative-ion electrospray mass spectra of **4b** with CD in molar ratio 1:1. (a) first-order MS of **4b** with β-CD; (b) MS^2 of an ion at *m/z* 851; (c) first-order MS of **4b** with α-CD; (d) MS^2 of an ion at *m/z* 770. The assignments for observed signals are shown in brackets. The fragmented ion in tandem mass spectra is marked with a black down-facing triangle.

In contrast to NMR and ITC experiments, we detected signals related to the complexes of the dyes with α-CD. This cyclodextrin homologue has a smaller interior cavity than β-CD, and the formation of an ordinary inclusion complex at the adamantane or naphthalene binding site of the dyes is very unlikely. Non-specific aggregates that can be formed between dyes and α-CD should be significantly weaker than inclusion complexes with β-CD. The assumption of weak complexes concerts with a significantly less abundant peak of $[M^{2-}+\alpha\text{-CD}]^{2-}$ compared to the β-CD complex, as shown in Figure 5c. The quantification of the binding strength of such weak complexes using NMR or ITC was disabled due to very small changes in chemical shifts within titrations and negligible interaction enthalpy, respectively. Therefore, we analysed the dependence of the ion yield (*IY*) on CID amplitude [36] to distinguish between the two types of supramolecular aggregates. The calculations used for constructing the graph in Figure 6 are

given in detail in the supplementary material. Briefly, ion yields of $[M^{2-}+CD]^{2-}$ were taken into account and initial values (*IY* for CID amplitude = 0) for all experiments with β-CD were set to unity. The initial abundance of the $[M^{2-}+\alpha\text{-CD}]^{2-}$ ion was then taken in respect of the corresponding β-CD complex. Figure 6 shows the two distinctly shaped curves that were observed for β-CD and α-CD complexes, respectively. The ion yield of the α-CD complexes is inconsiderable for CID amplitudes higher than 0.35 for both of the examined dyes, whereas significant amounts of analogical ions can be observed up to the CID value of 0.65 for β-CD complexes. The CCE, i.e. the value of CID amplitude providing 50% fragmentation efficiency, is another parameter that is widely used to compare aggregate stability [36]. Figure 6 clearly shows that $CCE_{\beta\text{-CD}}$ is approximately 0.41 for both dyes, whereas $CCE_{\alpha\text{-CD}}$ is 0.26. In other words, higher energy is needed for the complete dissociation of both β-CD complexes. This observation concerts with the assumption that α-CD complexes have significantly lower stability related to their exclusion nature.

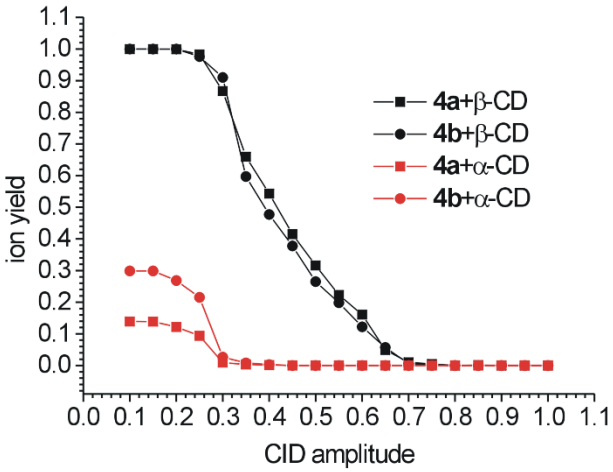

Figure 6 CID experiments distinguishing α-CD and β-CD complexes.

Subsequently, we performed mass spectrometry experiments with CB7 and CB8. In the negative-ion first-order mass spectra of equimolar mixtures of our dyes with CB7/8, we observed two doubly negative-charged ions at *m/z* 283.9 (molecular dianion of the

corresponding guest), *m/z* 865.1 (for CB7 mixtures) and *m/z* 948.2 (for CB8 mixtures). According to tandem mass spectrometry experiments, we assigned signals at *m/z* 865 and *m/z* 948 as doubly charged guest anion complexed with CB7 and CB8, respectively. Under the CID treatment, the neutral loss of the host molecule led to the formation of a doubly charged ion at *m/z* 283.9 in all cases (for spectra, see Figures S15–S20).

4. Conclusions

We prepared new azo dyes modified with lipophilic adamantane cage moiety. To the best of our knowledge, this is the first example of a supramolecular study on azo dyes bearing adamantane substituent, i.e. a well-known supramolecular guest entity and synthetically feasible structure that allows the dye to be incorporated into supramolecular systems via specific host–guest interactions. We then tested the supramolecular properties of these dyes on cyclodextrins and cucurbit[*n*]urils using NMR, MS and titration calorimetry. Both dyes formed 1:1 inclusion complexes with β-CD, CB7 and CB8. In all complexes, adamantane moiety was buried inside the macrocyclic host cavity, according to NMR. The dyes formed weak complexes with α-CD, most likely in a non-specific external manner as demonstrated using mass spectrometry. Association constants *K* were determined via titration calorimetry. While *K* values with CB7 and CB8 reflected the well-known behaviour of adamantane derivatives towards CB*n*s, the stability of complexes with β-CD was surprisingly high, rivalling the most stable complexes described so far [33]. We attributed these high affinities to additional non-specific interactions between the polar cyclodextrin rim and the polar part of the dye molecule. Finally, we demonstrated that complexation of the dyes with CB7 can be used to efficiently remove the dye from the solution due to the low solubility of the complex, even if competing β-CD is present.

Declaration of competing interest

The authors declare that they have no known competing financial interests or personal relationships that could have appeared to influence the work reported in this paper.

CRediT authorship contribution statement

Filip Zatloukal: Validation, investigation, writing – original draft, funding acquisition. **Eva Achbergerová**: Investigation. **David Gergela**: Validation, investigation, writing – original draft. **Zdeňka Prucková**: Investigation, methodology, writing – review and editing. **Lenka Dastychová**: Writing – original draft, writing – review and editing, visualisation. **Michal Rouchal**: Methodology, investigation, writing – original draft, writing – review and editing, visualisation. **Robert Vícha**: Conceptualisation, methodology, investigation, writing – original draft, writing – review and editing, visualisation, supervision, project administration.

Acknowledgement

The financial support of this work by the Internal Funding Agency of Tomas Bata University in Zlín, project IGA/FT/2021/001, is gratefully acknowledged.

References

[1] Hunger K. Industrial dyes: Chemistry, properties, applications. Wenheim: Wiley-VCH 2003, ISBN 3-527-30426-6.

[2] Ashutosh PND, Mehrotra JK. Azo dyes as metallochromic indicators. Colourage 1979;26:25.

[3] Athey RD. Free radical initiator basics. Eur Coat J 1998;3:146.

[4] Sandborn WJ. Rational selection of oral 5-aminosalicylate formulations and prodrugs for the treatment of ulcerative colitis. Am J Gastroenterol 2002;97:2939–41. https://doi.org/10.1111/j.1572-0241.2002.07092.x

[5] (a) Cisnetti F, Balardini R, Credi A, Gandolfi MT, Masiero S, Negri F, Pieraccini S, Spada GP. Photochemical and electronic properties of conjugated bis(azo) compounds: An experimental and computational study. Chem Eur J 2004;10:2011–21. https://doi.org/10.1002/chem.200305590; (b) Chomicki D, Kharchenko O, Skowronski L, Kowalonek J, Kozanecka-Szmigiel A, Szmigiel D, Smokal V, Krupka O, Derkowska-Zielinska B. Physico-Chemical and Light-Induced Properties of Quinoline Azo-dyes Polymers. Int J Mol Sci 2020; 21:5755. https://doi.org/10.3390/ijms21165755; (c) Derkowska-Zielinska B, Skowronski L, Sypniewska M, Chomicki D, Smokal V, Kharchenko O, Naparty M, Krupka O. Functionalized polymers with strong push-pull azo chromophores in side chain for optical application. Opt Mater 2018; 85:391–98. https://doi.org/10.1016/j.optmat.2018.09.008; (d) Derkowska-Zielinska B, Gondek E, Pokladko-Kowar M, Kaczmarek-Kedziera A, Kysil A, Lakshminarayana G, Krupka O. Photovoltaic cells with various azo dyes as components of the active layer. Sol Energy 2020; 203:19–24. https://doi.org/10.1016/j.solener.2020.04.022

[6] Beharry AA, Wooley GA. Azobenzene photoswitches for biomolecules. Chem Soc Rev 2011; 40:4422–47. https://doi.org/10.1039/c1cs15023e

[7] Ikeda T, Tsutsumi O. Optical switching and image storage by means of azobenzene liquid-crystal films. Science 1995;268:1873. https://doi.org/10.1126/science.268.5219.1873

[8] (a) Feringa BL, van Delden RA, Koumura N, Geertsema EM. Chiroptical molecular switches. Chem Rev 2000; 100:1789–1816. https://doi.org/10.1021/cr9900228; (b) Crespi S, Simeth NA, König B. Heteroaryl azo dyes as moleculat photoswitches. Nature Rev Chem 2019;3:133–46. https://doi.org/10.1038/s41570-019-0074-6

[9] Murakami H, Kawabuchi A, Kotoo K, Kutinake M, Nakashima N. A light-driven molecular shuttle based on a rotaxane. J Am Chem Soc 1997;119:7605–13. https://doi.org/10.1021/ja971438a

[10] Banerjee IA, Yu L, Matsui H. Application of host–guest chemistry in nanotube-based device fabrication: Photochemically controlled immobilization of azobenzene nanotubes on patterned α-CD monolayer/au substrates via molecular recognition. J Am Chem Soc 2003;125:9542–3. https://doi.org/10.1021/ja0344011

[11] Crano JC, Guglielmetti R. Organic photochromic and thermochronic compounds. New York: Plenum Press 1999, ISBN 0-306-45883-7.

[12] (a) Huang B-Y, Chen T-H, Chen T-Y, Lin J-D, Lin T-H, Kuo C-T. A planar fresnel lens in reflection type based on azo-dye-doped cholesteric liquid crystals fabricated by photo-alignment. Polymers 2020;12:2972. https://doi.org/10.3390/polym12122972; (b) Mohamed-Smati SB, Faraj FL, Becheker I, Berredjem H, Bideau F, Hamdi M, Dumas F, Rachedi Y. Synthesis, characterization and antimicrobial activity of some new azo dyes derived from 4-hydroxy-6-methyl-*2H*-pyran-2-one and its dihydro derivative. Dyes Pigm 2021;188:109073. https://doi.org/10.1016/j.dyepig.2020.109073; (c) Roik NV, Belyakova LA, Dziazko MO. Solubilization of azo dyes by cetyltrimethylammonium bromide micelles as structure control factor at synthesis of ordered mesoporous silicas. J Mol Liq 2021;328:115451. https://doi.org/10.1016/j.molliq.2021.115451; (d) Demirçali A, Karci F, Sari F. Synthesis and absorption properties of five new heterocyclic disazo dyes containing pyrazole and pyrazolone and their acute toxicities on the freshwater amphipod *Gammarus roeseli*. Color Technol 2021. https://doi.org/10.1111/cote.12530; (e) Mamatioğlu F, Üzer A, Erças E, Apak R. Development of a gold nanoparticles-based colorimetric sensor for the indirect determination of ammonium dinitramide and tetryl. Talanta 2021;226:122187. https://doi.org/10.1016/j.talanta.2021.122187

[13] Sha Y, Mathew I, Cui Q, Clay F, Gao F, Zhang X, Gu Z. Rapid degradation of azo dye methyl orange using hollow cobalt nanoparticles. Chemosphere 2016;144:1530–5. https://doi.org/10.1016/j.chemosphere.2015.10.040

[14] Loftsson T, Jarho P, Másson M, Järvinen T. Cyclodextrins in drug delivery. Expert Opi Drug Deliv 2005;2(2):335–51. https://doi.org/10.1517/17425247.2.1.335

[15] Tiwari G, Tiwari R, Rai AK. Cyclodextrins in delivery systems: Applications. Journal of Pharmacy and Bioallied Sciences 2010;2(2):72–9. https://doi.org/10.4103/0975-7406.67003

[16] Horský J, Jindřich J. Cyklodextriny ve světě polymerů. *Chem Listy* 2013;107:769–76.

[17] Ali I, Aboul-Einen HY. Chiral Pollutants: Distribution, toxicity and analysis by chromatography and capillary electrophoresis. Hoboken: J. Wiley 2004, ISBN: 978-0-470-86780-8.

[18] Mock WL. Comprehensive supramolecular chemistry 1996;2:477–93.

[19] Lagona J, Mukhopadhyay P, Chakrabarti S, Isaacs L. The cucurbit[*n*]uril family. Angew Chem Int Ed 2005;44:4844–70. https://doi.org/10.1002/anie.200460675

[20] (a) Assaf KI, Nau WM. Cucurbiturils: From synthesis to high-affinity binding and catalysis. Chem So. Rev 2015;44:394−418, https://doi.o□/10.1039/C4CS00273C; (b) Ba□ow SJ, Kas□a S, Rowland MJ, d□l Ba□io J, Scherman OA. Cucurbituril-based molecular recognition. Chem Rev 2015;115:12320–406. https://doi.org/ 10.1021/acs.chemrev.5b00341

[21] Tomatsu I, Hashidzume A, Harada A. Photoresponsive hydrogel system using molecular recognition of α-cyclodextrin. Macromolecules 2005;38:5223–7. https://doi.org/10.1021/ma050670v

[22] Hamon F, Blaszkiewicz C, Buchotte M, Banaszak-Léonard E, Bricout H, Tilloy S, Monflier E, Cézard Ch, Bouteiller L, Len Ch, Djedaini-Pilard F. Synthesis and characterization of a new photoinduced switchable β-cyclodextrin dimer. Beilstein J Org Chem 2014;10:2874–85. https://doi.org/ 10.3762/bjoc.10.304

[23] Liu X, Wang K-R, Rong R-X, Liu M-H, Wang Q, Li X-L. Host-guest controlled assembly and recognition of perylene bisimide-based glycocluster with cyclodextrin. Dyes Pigm 2020;174:108043. https://doi.org/10.1016/j.dyepig.2019.108043

[24] Benčić P, Mandić L, Džeba I, Bujak IT, Biczók L, Mihaljević B, Mlinarić-Majerski K, Weber I, Basarić N. Application of 4-amino-*N*-adamantylphthalimide solvatochromic dye for fluorescence microscopy in selective visualization of lipid droplets and mitochondria. Sens Actuators B 2019;286:52–61. https://doi.org/10.1016/j.snb.2019.01.102

[25] (a) Liu T, Liu X, Zhang Y, Bondar MV, Fang Y, Belfield KD. Far-red- to NIR-emitting adamantyl-functionalized squaraine dye: J-aggregation, dissociation, and cell imaging. Eur J Org Chem 2018;4095–102, https://doi.org/10.1002/ejoc.201800584; (b) Xu W, Zhu X, Wang G, Sun C, Zheng Q, Yang H, Fu N. Host–guest assembly of adamantyl tethered squaraine in β-cyclodextrin for monitoring pH in living cells. RSC Adv 2014;4:52690–3. https://doi.org/10.1039/C4RA08506J

[26] Chen J, Luo S, Xu D, Xue Y, Huang H, Wan Q, Liu M, Zhang X, Wei Y. Fabrication of AIE-active amphiphilic fluorescent polymeric nanoparticles through host–guest interaction. RSC Adv 2016;6:54812–9. https://doi.org/10.1039/C6RA08677B

[27] (a) Xie X, Li X, Luo H, Lu H, Chen F, Li W. The adsorption of reactive blue 19 dye onto cucurbit[8]uril and cucurbit[6]uril: An experimental and theoretical study. J Phys Chem B 2016;120:4131–42. https://doi.org/10.1021/acs.jpcb.6b035 65; (b) He S, Sun X, Zhang H. Influence of the protonation state on the binding mode of methyl orange with cucurbiturils. J Mol Struct 2016;1107:182–8. https://doi.org/10.1016/j.molstruc.2015.11.039; (c) Cicolani RS, Souza LRR, de Santana Dias GB, Goncalves JMR, dos Santos Abrahao I, Silva VM, Demets GJF. Cucurbiturils for environmental and analytical chemistry. J Incl Phenomen Macrocycl Chem 2021;99:1–12. https://doi.org/10.1007/s10847-020-00999-8

[28] Saifi A, Joseph JP, Singh AP, Pal A, Kumar, K. Complexation of an azo dye by cyclodextrins: A potential strategy for water purification. ACS Omega 2021;6:4776–82. https://doi.org/10.1021/acsomega.0c05684

[29] (a) Vícha R, Rouchal M, Kozubková Z, Kuřitka I, Marek R, Branná P, Čmelík R. Novel adamantane-bearing anilines and properties of their supramolecular complexes with β-cyclodextrin. Supramol Chem 2011;23:663–77. https://doi.org/10.1080/10610278.2011.593628; (b) Vícha R, Kuřitka I, Rouchal M, Ježková V, Zierhut A.

Directing effects in nitration of 1-adamantyl bearing aromatic ketones. ARKIVOC 2009;(*xii*):60–80. https://doi.org/10.3998/ark.5550190.0010.c06

[30] Rekharsky MV, Mori T, Yang C, Ko YH, Selvapalam N, Kim H, Sobransingh D, Kaifer AE, Liu S, Isaacs L, Chen W, Moghaddam S, Gilson MK, Kim K, Inoue Y. A synthetic host-guest system achieves avidin-biotin affinity by overcoming enthalpy–entropy compensation. Proc Natl Acad Sci USA 2007;104:20737–42. https://doi.org/10.1073/pnas.0706407105

[31] Anderson S, Claridge TDW, Anderson HL. Azo-dye rotaxanes. Angew Chem Int Ed Engl 1997;36:1310–3. https://doi.org/10.1002/anie.199713101

[32] (a) Bártová K, Císařová I, Lyčka A, Dračínský M. Tautomerism of azo dyes in the solid state studied by ^{15}N, ^{14}N, ^{13}C and ^{1}H NMR spectroscopy, X-ray diffraction and quantum-chemical calculations. Dyes Pigm 2020;178:108342. https://doi.org/10.1016/j.dyepig.2020.108342; (b) Deneva V, Lyčka A, Hristova S, Crochet A, Fromm KM, Antonov L. Tautomerism in azo dyes: Border cases of azo and hydrazo tautomers as possible NMR reference compounds. Dyes Pigm 2019;165:157–63. https://doi.org/10.1016/j.dyepig.2019.02.015; (c) Antonov L. Tautomerism in azo and azomethyne dyes: When and if theory meets experiment. Molecules 2019;24:2252. https://doi.org/10.3390/molecules24122252; (d) Lyčka A. ^{15}N, ^{13}C and ^{1}H NMR spectra and azo-hydrazone tautomerism of some dyes prepared by coupling of 1-naphthalenediazonium salt. Dyes Pigm 1999;43:27–32. https://doi.org/10.1016/S0143-7208(99)00032-7; (e) Lyčka A, Macháček V. ^{13}C and ^{15}N-NMR studies of the azo-hydrazone tautomerism of some azo dyes. Dyes Pigm 1986;7:171–85. https://doi.org/10.1016/0143-7208(86)85008-2

[33] (a) Schibilla F, Voskuhl J, Fokina NA, Dahl JEP, Schreiner PR, Ravoo BJ. Host–guest complexes of cyclodextrins and nanodiamonds as a strong non-covalent binding motif for self-assembled nanomaterials. Chem Eur J 2017;23:16059–65. https://doi.org/10.1002/chem.201703392; (b) Tomeček J, Čablová A, Hromádková A, Novotný J, Marek R, Durník I, Kulhánek P, Prucková Z, Rouchal M, Dastychová L, Vícha R. Modes of micromolar host–guest binding of β-cyclodextrin complexes revealed by NMR spectroscopy in salt water. J Org Chem 2021;86:4483–96. http://dx.doi.org/10.1021/acs.joc.0c02917

[34] Branná P, Černochová J, Rouchal M, Kulhánek P, Babinský M, Marek R, Nečas M, Kuřitka I, Vícha R. Cooperative binding of cucurbit[*n*]urils and β-cyclodextrin to heteroditopic imidazolium-based guests. J Org Chem 2016;81:9595–604. https://doi.org/10.1021/acs.joc.6b01564

[35] (a) Moghaddam S, Yang C, Rekharsky M, Ko YH, Kim K, Inoue Y, Gilson MK. New ultrahigh affinity host−guest complexes of cucurbit[7]uril with bicyclo[2.2.2]octane and adamantane guests: Thermodynamic analysis and evaluation of M2 affinity calculations. J Am Chem Soc 2011;133:3570–81. https://doi.org/10.1021/ja109904u; (b) Liu SM, Ruspic C, Mukhopadhyay P, Chakrabarti S, Zavalij PY, Isaacs L. The cucurbit[*n*]uril family: Prime components for self-sorting systems. J Am Chem Soc 2005;127:15959–67. https://doi.org/10.1021/ja055013x; (c) Cao LP, Šekutor M, Zavalij PY, Mlinarić-Majerski K, Glaser R, Isaacs L. Cucurbit[7]uril·guest pair with an attomolar dissociation constant. Angew Chem Int Ed 2014;53:988–93. https://doi.org/10.1002/anie.201309635; (d) Šekutor M, Molčanov K, Cao LP, Isaacs L, Glaser R, Mlinarić-Majerski K. Design, synthesis, and X-ray structural analyses of diamantane diammonium salts: Guests for cucurbit[*n*]uril (CB[*n*]) hosts. Eur J Org Chem 2014;2533–42. https://doi.org/10.1002/ejoc.201301844; (e) Jelínková K, Surmová H, Matelová A, Prucková Z, Rouchal M, Dastychová L, Nečas M, Vícha R. Cubane arrives on the cucurbituril scene. Org Lett 2017;19:2698–701. https://doi.org/10.1021/acs.orglett.7b01029

[36] Memboeuf A, Nasioudis A, Indelicato S, Pollreisz F, Kuki Á, Kéki S, Brink van den OF, Vékey K, Drahos L. Size effect on fragmentation in tandem mass spectrometry. Anal Chem 2010;82:2294–302. https://doi.org/10.1021/ac902463q